A Sixfold-Resolution Light-Field Display Using a Field-Sequential Color LCD and Optical Super-Resolution

Yifan Ding*, Xinni Xie*, Qimeng Wang*, Feiyi Wu*, Bo-Ru Yang*, and Zong Qin*

***School of Electronic and Information Technology, Sun Yat-Sen University, Guangzhou, China**

Abstract

Light field displays (LFDs) suffer from low resolution. This study first adopts a color-filter-less field-sequential-color LCD to provide a tripled resolution. Next, the LFD is demonstrated to work through incoherent synthetic apertures, based on which varying aliasing is introduced into a microlens array's apertures for a super-resolution of approximately two times.

Author Keywords

Light field display; field sequential color; super-resolution.

1. Introduction

The light field display (LFD) is promising to alleviate the vergence-accommodation conflict (VAC) for true-3D display [1]. The typical implementation adopts a microlens array (MLA) as its light modulator to manipulate light rays emitted from a display panel to reconstruct realistic 3D scenes, as Fig. 1 shows. LFDs provide computationally adjustable depth, compact volume, and feasible hardware. Originating from light field photography, the LFD contains two main steps: pickup and display. In the pickup stage, rays carrying spatial and angular information are manipulated by a microlens array (or a pinhole array), captured by a camera array, and recorded as an elemental image array (EIA). In the display process, a display panel replaces the camera array to achieve an inverted light path.

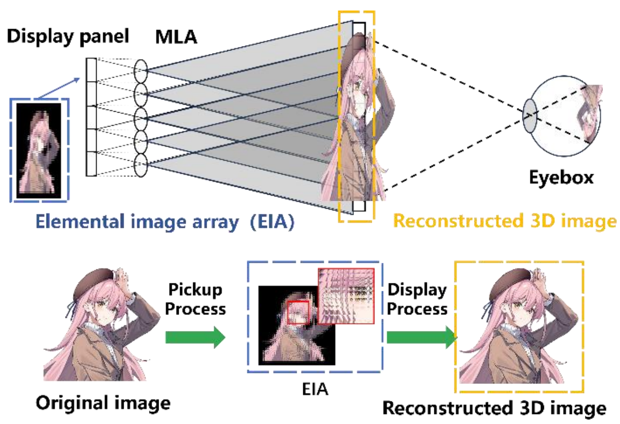

Fig. 1. Working principle of light field displays

However, this working principle causes a sharp decrease in spatial resolution because the limited resolution of the display panel must be allocated to spatial and angular resolution [2]. The sacrifice in spatial resolution is one of the biggest hindrances to LFDs. For instance, near-eye LFDs that attract significant attention for VR/AR headsets are still far from the human resolution limit (30~60 pixels/degree).

A popular approach to resolution enhancement for LFDs is dynamic super-resolution (SR) based on time-multiplexing, e.g., moving the display panel using a polarization-sensitive MLA with a polarization rotator [3]. Wang et al. [4] utilized a digitally switchable shutter array to achieve such dynamic SR. However, these methods require a complicated dynamic light modulator (e.g., liquid crystal lens). Besides, the enhancement cannot exceed twofold, limited by the pixel shape's frequency spectrum [5]. Therefore, an over-twofold-resolution approach for LFDs in a computational manner is needed.

This study combines two strategies to break the twofold resolution enhancement without using dynamic light modulators. The first effort is natively increasing the display panel's resolution using a field sequential color (FSC) LCD. The FSC-LCD removes the color filter array but accomplishes color mixing by rapidly flashing chromatic subframes. As a result, the spatial resolution is tripled, as Figs. 2(a) and (b) show. The color breakup issue of FSC displays should be a concern, which has been well addressed by our previous studies using deep learning [6].

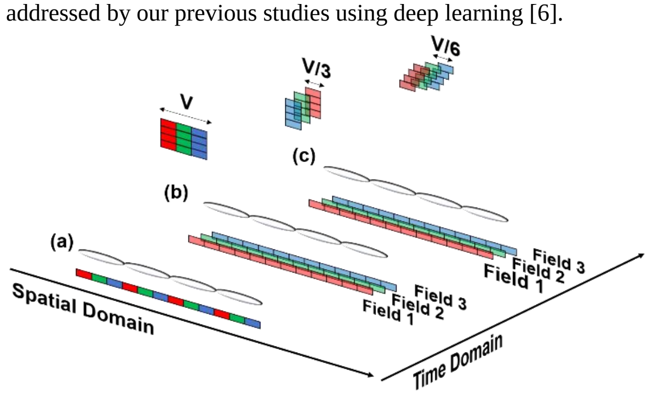

Fig. 2. LFD implemented with (a) the traditional architecture, (b) an FSC-LCD, and (c) super-resolution.

The second effort exploits the incoherent synthetic aperture (ISA) working principle of LFDs [7]. ISA refers to the fact that the computational focus cue of LFDs is achieved by incoherently synthesizing plural subviews (i.e., elemental images). This can introduce subpixel-level sampling shifts into different subviews. As shown in Fig. 2(c), the homogeneous pixels on the FSC-LCD are synthesized with sampling shifts, which may equivalently increase the sampling rate. Consequently, synthetic apertures with varying aliasing may break the Nyquist frequency for SR with no dynamic components.

Combining the above two approaches, we build an LFD prototype based on a 2.1-inch FSC-LCD, which provides a 2.3K-by-2.3K resolution free of color filters. SR that introduces elaborately displaced aliasing into different microlenses further doubles the resolution.

2. Method

Fig. 3 shows how elemental images are synthesized through apertures in an LFD. In an ideal circumstance shown in Fig. 3(a), the elemental images overlap perfectly, so the pixel pitch p determines the resolution. However, actual pixels and lenslets may introduce subpixel-level shifts between apertures, as shown in Fig. 3(b). These subpixel-level shifts are usually undesired, whereas a study on light field microscopy [8] demonstrates that such shifts introduce varying aliasing in different elemental images, which can be utilized to retrieve information beyond the Nyquist frequency, $f_{Nyquist}$, of $1/(2p)$.

ISSN 0097-996X/25/5602-0805-$1.00 © 2025

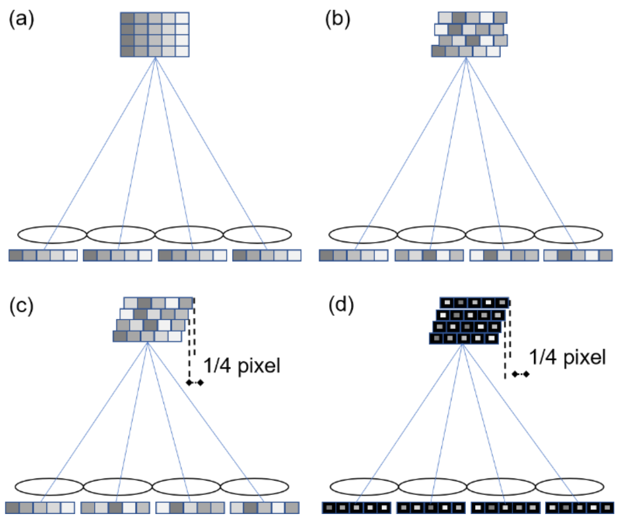

Fig. 3. (a) Ideal synthesis of EIA. (b) Elemental images with undesired sampling shifts. (c) Controlled sampling shifts of 1/N pixel pitch. (d) Same as (c) except for a smaller pixel fill factor.

According to a conclusion from our previous study [9], the sampling shift ε between adjacent lenslets is constant, determined by the structural parameters of an LFD (lens pitch, pixel size, and image depth). Intuitively, as Fig. 3(c) shows, the optimal sampling shift is 1/N pixel pitch *p*, which can obtain an N-fold oversampling rate (N: aperture number). Differently, the microscopy study [8] utilized the sampling shift for super-resolution but did not control the shift magnitude, not reaching an N-fold bandwidth from N elemental images.

In addition, continuous optical signals must be reconstructed by the shape of pixels after sampling, which is widely known as the zero-order hold (ZOH) process in a 2D display. Therefore, the pixel's square shape limits the overall bandwidth to less than $2f_{Nyquist}$ because its frequency spectrum, a sinc function, has its zero point at $2f_{Nyquist}$. Fortunately, an actual display's fill factor is less than 100%. As Fig 3(d) shows, smaller emitting areas are stitched for an ideally multiplied resolution. Therefore, under an oversampling rate of N when synthesizing through N apertures, the overall resolution can be N times if the emitting area occupies 1/N of a pixel pitch.

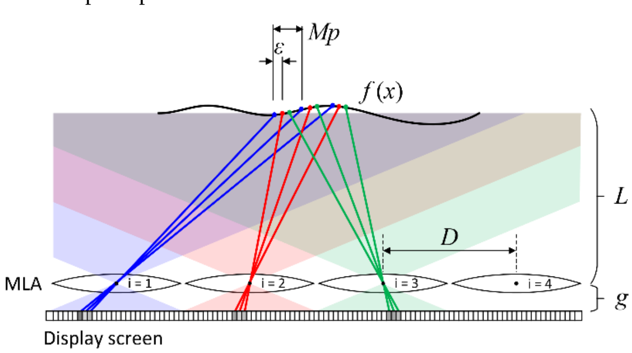

Fig. 4. Image formation via elemental image synthesis in an LFD. The three groups of rays with RGB colors denote sampling positions corresponding to three lenslets.

The following discussion rigorously analyzes the role of the sampling shift ε regarding an LFD's structural parameters. Fig. 4 shows a continuous signal *f*(*x*) incoherently synthesized by elemental images under several lenslets, which equals to a summation of multiple ZOH processes, as given by Eq. (1). Besides, the point spread function PSF(*x*) applied by the lenslet is also considered.

$$f_{\text{synthesis}}(x) = \sum_{i=1}^{N}\left[f(x)\cdot\text{comb}\left(\frac{x-\varepsilon_i}{p}\right)\right] * \text{rect}\left(\frac{x}{p}\right) * \text{PSF}(x) \quad \textbf{, (1)}$$

where comb(*x*/*p*) is the Dirac comb with an interval *p* for sampling; rect(*x*/*p*) is the rectangular function with a width *p* for reconstruction; * denotes convolution. The sampling shift ε_i inside the comb term is determined by the structural parameters and accumulates with lenslets, as Eq. (2) gives.

$$\varepsilon = k \cdot D\left(1+\frac{g}{L}\right) \bmod p \,, \tag{2}$$

where mod: modulo operation; g and L: distances of the image plane and the display screen to the MLA (see Fig. 4); *k*: lenslet number between two sampling rays (for adjacent lenslets, *k* = 1).

We apply the Fourier transform on the synthesized elemental images to analyze the effect of sampling shift. Eq. (3) gives its frequency spectrum.

$$\begin{aligned} F_{synthetic}(f) &= \mathscr{F}\left\{\sum_{i=1}^{N}\left[f(x)\cdot\text{comb}\left(\frac{x-\varepsilon_i}{p}\right)\right] * \text{rect}\left(\frac{x}{p}\right) * \text{PSF}(x)\right\} \\ &= \text{OTF}(f)\cdot\text{sinc}(pf)\cdot\sum_{i=1}^{N} F(f) * [\text{comb}(pf)e^{-i2\pi f \varepsilon_i}] \\ &= \text{OTF}(f)\cdot\text{sinc}(pf)\cdot G(f) \end{aligned} \tag{3}$$

where OTF(*f*) is the optical transfer function, a linear decay with its cutoff at D/(λg) under a diffraction-limited assumption.

From Eq. (3), three factors affect the overall bandwidth: (i) the OTF term from optical imaging, (ii) the sinc term from the square pixel shape, and (iii) G(*f*), namely the summation in the second row, which is a synthesis of several groups of spectrum replications modified by sampling shifts. The OTF term can be omitted because the diffraction-limited cutoff frequency is usually much higher than the Nyquist frequency. G(*f*), called the incoherent synthetic aperture (ISA) term here, is critical to oversampling because it incorporates varying aliasing through different subpixel-level shifts. Finally, the sinc term causes the overall bandwidth to vanish beyond its first zero point at 1/*p*.

$$D\left(1+\frac{g}{L}\right) = \left(Z+\frac{1}{N}\right)p \tag{4}$$

The most favorable case is that the sampling shift ε between adjacent lenslets is p/N, as Eq. (4) gives. Z denotes how many pixels lie between two adjacent homogeneous pixels, which can be arbitrarily selected.

We assume N = 4 and calculate the ISA spectrum. With an expected sampling shift of p/4, three out of four spectrum replicas are eliminated for a 4-fold sampling rate, as Fig. 5(a) shows. On the other hand, spectrum replicas are suppressed but not canceled out with other sampling shifts, like 0.12p in Fig. 5(b), still producing aliasing to a certain extent.

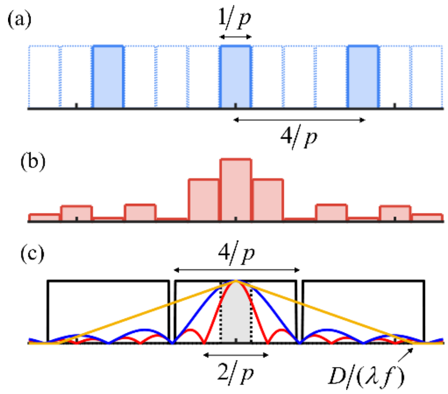

Fig. 5. ISA spectrum produced by (a)an ideal sampling shift of p/4 and (b) an imperfect shift of 0.12p. (c) Input spectrum with an aliasing-free bandwidth of $4f_{Nyquist}$ (black), sinc terms from 100% (red) and 50% (blue) fill factors, as well as the OTF (yellow).

The overall frequency spectrum of the reconstructed image is given in Fig. 5(c), considering the OTF term and two sinc terms corresponding to two fill factors (100% and 50%). The smaller fill factor produces a broader sinc term; thus, the ultimate bandwidth is expanded beyond $2f_{Nyquist}$. The particular value should be determined considering the minimum acceptable contrast sensitivity [10]. We can now conclude that the overall resolution can reach at least twofold under a 4-fold oversampling configuration.

3. Result

We build a near-eye LFD prototype based on a 2.1-inch FSC-LCD with a 2.3K-by-2.3K resolution and an MLA (pitch: 1 mm; focal length: 3.3 mm). Fig. 6(a) shows the experimental setup, where a Fresnel lens from the Meta Quest 2 headset is adopted in front of the MLA as an eyepiece. A Fujifilm X-S10 camera imitates a human observer. The oversampling rate N is set to four.

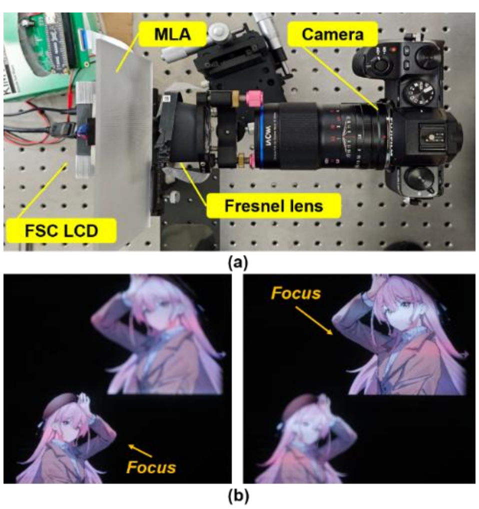

Fig. 6. (a) LFD using the FSC-LCD and a Fresnel lens; (b) reconstructed 3D image with two depth planes

For verifying 3D reconstruction, two depth planes are rendered, as Fig. 6(b) shows. The focus cue is observed by focusing on either depth plane while the other exhibits defocus. Next, the depth plane in the lower left object is selected to verify the super-resolution. The USAF-1951 chart is adopted to evaluate the resolution enhancement, as shown in Fig. 7.

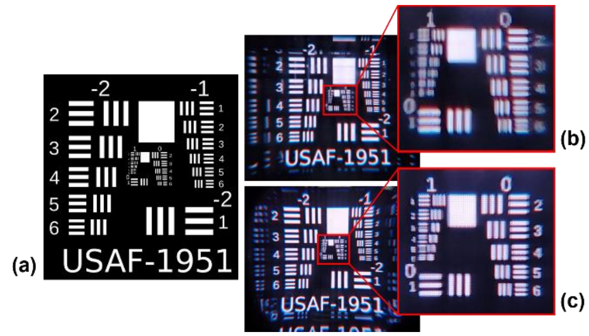

Fig. 7. Experiment to verify SR: (a) original USAF chart; reconstructed image without (b) and with (c) SR.

According to the minimum distinguishable line pairs in Figs. 7(b) and (c), the proposed SR method achieves a 1.87 times resolution. Compared with the ideal gain larger than two, the experimental result is somewhat lower because of the difficulty in aligning the MLA with the FSC-LCD at a subpixel-level precision. Distortion can be seen in large fields because no image wrapping is performed regarding the optical distortions of the Fresnel lens. Considering the triple resolution brought by the FSC-LCD, the proposed LFD can approximately achieve a sixfold resolution.

4. Conclusion

This study proposed a sixfold-resolution light field display using an FSC-LCD combined with the optical SR method. In addition to the native resolution enhancement brought by the FSC technology, the incoherent synthetic aperture principle in LFDs was exploited. We proposed that elaborated introduced aliasing varying with apertures can computationally enhance the resolution around twofold. We consider the combination of the two methods a promising approach to high-resolution LFDs.

5. References

1. B. Javidi, A. Carnicer, J. Arai, et al., "Roadmap on 3Dintegral imaging: Sensing, processing, and display," Opt. Express **28**, 32266-32293 (2020).
2. Z. Qin et al., "Resolution-enhanced light field displays by recombining subpixels across elemental images," Opt. Lett. **44**, 2438-2441 (2019).
3. T. Zhan, J. Xiong, G. Tan, Y.-H. Lee, J. Yang, S. Liu, and S.-T. Wu, "Improving near-eye display resolution by polarization multiplexing," Opt. Express **27**, 15327 (2019).
4. T. Zhan, J. Xiong, G. Tan, Y.-H. Lee, J. Yang, S. Liu, and S.-T. Wu, "Improving near-eye display resolution by polarization multiplexing," Opt. Express **27**, 15327 (2019).
5. Y. Ding, Y. Qiu, Q. Wang, Y. Cheng, Y. Liu, B.-R. Yang, and Z. Qin, "Exploiting incoherent synthetic apertures in integral imaging for optical super-resolution," Opt. Lett. **49**, 5679 (2024).
6. Z. Wang, G. Zou, Y. Shen, B.-R Yang, and Z. Qin, "Deep learning-based real-time driving for 3-field sequential color displays with low color breakup and high fidelity," Opt. Express **31**, 17999 (2023).

7. J. Wu, Y. Guo, C. Deng, A. Zhang, H. Qiao, Z. Lu, J. Xie, L. Fang, and Q. Dai, "An integrated imaging sensor for aberration-corrected 3D photography," Nature **612**, 62 (2022).
8. A. Stefanoiu, G. Scrofani, G. Saavedra, M. Martínez-Corral, and T. Lasser, "What about computational super-resolution in fluorescence Fourier light field microscopy?" Opt. Express **28**(11), 16554 - 16568 (2020).
9. W. Yang, Y. Cheng, G. Zou, B. Yang, and Z. Qin, "Enhancing the spatial resolution of light-field displays without losing angular resolution by a computational subpixel realignment," Opt. Lett. **49**, 1 (2024).
10. Z. Qin, P.-J. Wong, W.-C. Chao, F.-C. Lin, Y.-P. Huang, and H.-P. D. Shieh, "Contrast-sensitivity-based evaluation method of a surveillance camera's visual resolution: improvement from the conventional slanted-edge spatial frequency response method," Appl. Opt. **56**(5), 1464–1471 (2017).